High-spin states in ^{207}At

T. P. Sjoreen,* U. Garg,† and D. B. Fossan
Department of Physics, State University of New York, Stony Brook, New York 11794
(Received 20 June 1980)

The properties of high-spin states in ^{207}At have been studied with the ^{204}Pb(^{6}Li,3n)^{207}At reaction. In-beam measurements with Ge(Li) and intrinsic Ge detectors of γ-γ coincidences, γ-ray angular distributions, pulsed-beam γ timing, and perturbed angular distributions with an applied magnetic field were made to determine a decay scheme, level energies, γ-ray multipolarities, spin-parity assignments, an isomeric lifetime, and a g factor. High-spin states up to $25/2\hbar$ were identified as either proton excitations of the ($N = 126$) ^{211}At nucleus coupled to the ^{204}Pb $Z = 82$ ground state or neutron excitations of ^{204}Pb coupled to the $(\pi h_{9/2})^3$ $9/2^-$ ground state of ^{211}At. Lifetime and g-factor measurements of the $25/2^+$ 2117-keV isomer, which yielded values of $\tau = 156(3)$ nsec and $g = 0.30(1)$, respectively, strongly support a $|(\pi h_{9/2})^3 9/2^-, (\nu f_{5/2})^{-1}(\nu i_{13/2})^{-1} 9^-; 25/2^+\rangle$ configuration for this level.

[NUCLEAR REACTIONS ^{204}Pb(^{6}Li, 3$n\gamma$), $E_{Li} = 34$ MeV; measured γ-γ coin, γ-$W(\theta)$, pulsed-beam γ timing, perturbed angular distributions; deduced levels, γ multipolarities, J^π, $T_{1/2}$, $B(E1)$, g.]

I. INTRODUCTION

Nuclei surrounding ^{208}Pb have been successfully interpreted in terms of shell model configurations of a few valence particles because of the good neutron $N = 126$ and proton $Z = 82$ shell closures. High-spin states in these nuclei are particularly simple to describe since the number of possible shell model configurations is severely limited. Fusion evaporation reactions induced by heavy ions along with in-beam γ-ray spectroscopy represent effective methods for populating such states and studying their decay modes. Recently several groups[1-8] have taken advantage of these methods to study the lighter mass ($N < 126$) trans-Pb nuclei of Bi, Po, At, and Rn, which are generally not accessible with light-ion ($A < 4$) induced reactions. The purpose of these studies has been to investigate the interaction between the valence proton structure defined by the ^{209}Bi, ^{210}Po, ^{211}At, and ^{212}Rn closed neutron-shell ($N = 126$) isotones and the neutron-hole excitations of the even-Pb isotopes ($Z = 82$).

The present ^{207}At measurements were motivated by earlier studies[4,5] of ^{209}At, which investigated the interaction between the two-neutron holes $(\nu)^{-2}$ of ^{206}Pb and the three-proton structure $(\pi)^3$ of ^{211}At. These measurements showed that, except for the first two excited levels, the yrast levels (those levels having the minimum energy for a given spin J) of ^{209}At have a close resemblence to those for ^{211}At. This indicated that these ^{209}At levels could be identified as the ^{206}Pb ground state coupled to $(\pi)^3$ excitations, which are known from ^{211}At to involve $(h_{9/2})^3$, $(h_{9/2})^2(f_{7/2})$, and $(h_{9/2})^2(i_{13/2})$ proton configurations. Although complete shell model calculations for ^{209}At are essentially impossible, because of the large three-particle two-hole basis required, relatively simple calculations based on first order perturbation theory[4] and a truncated shell model using ^{206}Pb as a core[5,9] were successful in describing the influence of the two-neutron holes on the measured transition matrix elements and on several of the energy levels. The purpose of the present study is to experimentally obtain the properties of high-spin states in ^{207}At, in order to compare them with those for ^{209,211}At, and to determine the extent to which the four-neutron hole structure of ^{204}Pb influences the ^{207}At level scheme. It is also important to follow the high-spin systematics of the $Z > 82$ nuclei to greater neutron deficiency in an effort to search for the onset of collectivity for specific proton configurations. Preliminary results from another study[7] extended these systematics to ^{205}At.

At the beginning of the present study the only available information on ^{207}At involved low-spin states which were populated by β decay of ^{207}Rn.[10] To investigate the high-spin states of ^{207}At, in-beam γ-ray measurements via the ^{204}Pb(^{6}Li, 3n) fusion evaporation reaction were made. A level scheme, including deduced J^π assignments, was determined, and the $\frac{25}{2}^+$ 2117-keV level was found to be isomeric. Lifetime and g-factor measurements for this level yielded values of $\tau = 156$ (3) nsec and $g = 0.30$ (1), which strongly support the interpretation of this state as the 9^- excitation of ^{204}Pb coupled to the ^{211}At ground state. Preliminary results of some of these measurements have been reported previously[11] and a brief presentation of the g-factor measurement has been made.[6]

In Sec. II, the techniques for the in-beam γ-ray measurements are briefly described; a more de-

 © 1981 The American Physical Society

tailed discussion is available in the ^{206}Pb(^{6}Li, $3n$) ^{209}At study.[4] The experimental results for ^{207}At are presented in Sec. III and in Sec. IV the level scheme is discussed in terms of the shell model and compared with ^{205,209,211}At.

II. EXPERIMENTAL PROCEDURE

Levels in ^{207}At were populated via the ^{204}Pb(^{6}Li, $3n$)^{207}At fusion evaporation reaction. For these measurements a 34 MeV ^{6}Li(3^{+}) beam, obtained from the Stony Brook FN Tandem Van de Graaff Accelerator, was incident on an enriched (>99%) ^{204}Pb foil which was 10 mg/cm^2 thick. For the g-factor measurement a thick enriched ^{208}Pb backing was added to stop the beam. Deexcitation γ rays were detected using both large volume Ge(Li) detectors and smaller planar Ge detectors; typical energy resolutions were 2.0-keV full width at half maximum (FWHM) at 1332 keV and 0.8-keV FWHM at 122 keV, respectively. Four types of experiments were carried out: (1) γ-γ coincidence, (2) γ-ray angular distribution, (3) pulsed beam-γ timing, and (4) time differential perturbed angular distribution measurements.

The γ-γ coincidence measurement, with two large coaxial Ge(Li) detectors, was carried out to identify the γ-ray cascades. The γ-ray angular distributions were measured in singles at four angles between 90° and 150° to determine the γ-ray multipolarities and spin information for the levels, as well as the γ-ray intensities I_γ. The photopeak areas were extracted, normalized for dead time and geometric effects, and fitted to $W(\theta) = I_\gamma(1 + A_2P_2 + A_4P_4)$, where $P_K(\cos\theta)$ are the Legendre polynomials. The pulsed-beam timing measurements were made to locate isomeric states and determine their lifetimes and decay modes. For the lifetime measurements, the beam was pulsed at repetition rates of 1 or 2 μ sec with a pulse time width of about 3 nsec. Both delayed γ-ray spectra for the entire energy range and time differential spectra for specific γ rays were obtained. To probe the nuclear wave function of the isomer at 2117 keV, its g factor was measured with the time differential perturbed angular distribution method. For this measurement, the beam was pulsed at a repetition rate of 1 μsec with a time width of ≤3 nsec. The magnetic field, which was applied perpendicular to the beam axis, was calibrated by a measurement of the g factor of the 8^{+} state of ^{210}Po; this was done via the ^{208}Pb(α, $2n$) reaction by rotating the target and bombarding the ^{208}Pb backing with 25.5 MeV α particles. Using $g = 0.914$ (1) for the 8^{+} state in ^{210}Po,[12] the applied field was determined to be $B = 12.6$ (1) kG. The decay γ rays were detected by two planar Ge detectors positioned at ±135° to the beam axis in a plane perpendicular to the applied field.

III. EXPERIMENTAL RESULTS

Fifteen γ rays were assigned to ^{207}At on the basis of the present ^{204}Pb(^{6}Li, $3n$) γ-ray measurement at $E_{\mathrm{Li}} = 34$ MeV. These γ rays are labeled in units of keV in Fig. 1. All the other strong γ rays in this spectrum, which are not labeled, were identified with the (^{6}Li, αn)^{205}Bi, (^{6}Li, $\alpha 2n$)^{204}Bi, and (^{6}Li, αp)^{205}Pb breakup reactions or with radioactive decay. At 34 MeV bombarding energy, all the other evaporation channels are weak compared to that for (^{6}Li, $3n$)^{207}At. The relative intensities

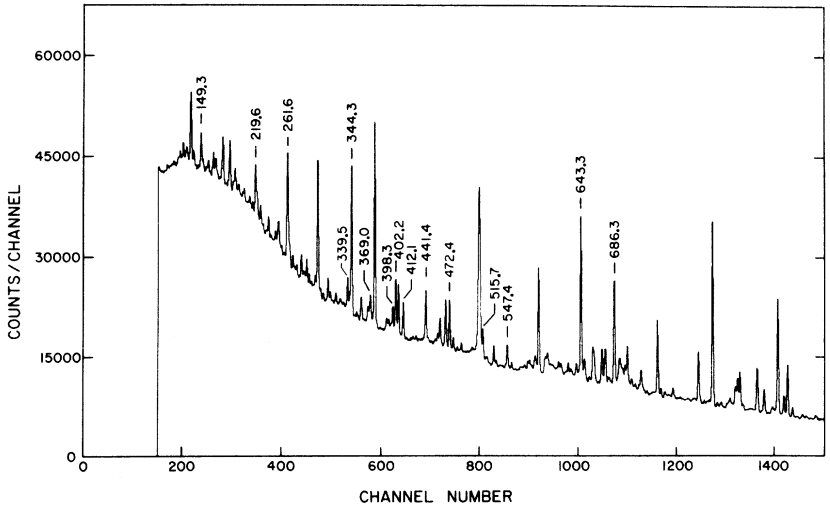

FIG. 1. A portion of the γ-ray spectrum observed with a Ge(Li) detector at 90° to the beam for the bombardment of a 10 mg/cm^2 ^{204}Pb target with 34 MeV ^{6}Li ions. The energies of the ^{207}At γ rays are given in units of keV.

observed for the various $^{204}Pb + ^{6}Li$ reaction channels are similar to those observed[4] for $^{206}Pb + ^{6}Li$ at 34 MeV.

The results of the γ-γ coincidence measurement are summarized in Table I, from which the level scheme for ^{207}At was constructed. The most prominent feature of the decay scheme is the γ-ray cascade from the 2117-keV level to the ground state, with branches occurring at the 1234-, 1085-, and 1055-keV levels. In Fig. 2, coincidence spectra for the 262-, 643-, and 686-keV γ rays of this cascade are shown. The 30-keV transition between the 1085- and 1055-keV levels is not observed in the γ-γ data; however, the inclusion of this trasition in the level scheme is suggested by the time differential measurement which will be discussed below.

The other feature of the ^{207}At level scheme is the cascade of three γ rays from the 1971-keV level to the 643-keV level. The 340-keV member of this cascade is tentatively assigned to the ^{207}At level scheme, as denoted by the dotted line in Fig. 3. Most of the intensity of this γ ray belongs to a ^{205}Bi transition.

All the γ rays listed in Table I except for the 344-keV γ ray were assigned to the ^{207}At level scheme in Fig. 3. The 344-keV γ ray is probably the transition from the $\frac{7}{2}^-$ level to the ground state in ^{207}At which has been observed in a study of the β decay of ^{207}Rn.[10]

From the pulsed beam-γ timing measurements, the 2117-keV level was discovered to be isomeric with a mean lifetime of $\tau = 156$ (3) nsec. Evidence

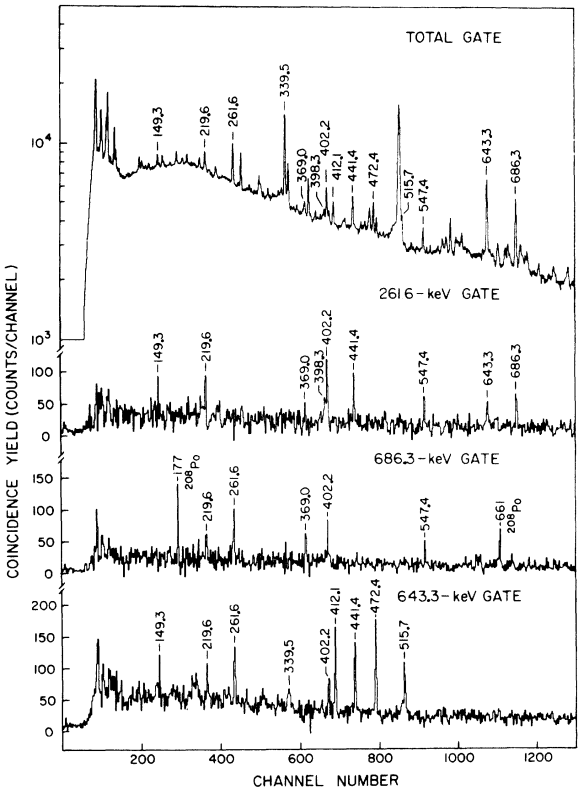

FIG. 2. γ-γ coincidence spectra from the $^{204}Pb(^{6}Li, 3n)^{207}At$ reaction observed with two Ge(Li) detectors for four γ-ray gates. The total gate spectrum is coincident with all γ rays from 50 to 1000 keV.

TABLE I. Results of γ-γ coincidence measurements for ^{207}At.

Gate energy (keV)	Coincident γ rays[a]
149.3	(441.4), (643.3)
219.6	(149.3), 261.6, 402.2, (643.3), (686.3)
261.6	149.3, 219.6, (369.0), 398.3, 402.2, 441.4, 547.4, 643.3, 686.3
339.5[b]	1001.2[^{205}Bi]
369.0	686.3
398.3	(261.6), 686.3
402.2	(149.3), 219.6, 261.6, 547.4, 643.3, 686.3
412.1	643.3
441.4	261.6, (402.2), 643.3
472.4	(339.5), 515.7, 643.3
515.7	472.4, 643.3
547.4	261.6, 402.2, 686.3
643.3	149.3, 219.6, 261.6, (339.5), 402.2, 412.1, 441.4, 472.4, 515.7
686.3	177.0[^{208}Po], (219.6), 261.6, 369.0, 402.2, 547.4, 661.0[^{208}Po]

[a] Parentheses around γ-ray energy indicate a weak coincidence.
[b] This γ ray is tentatively assigned to ^{207}At; most of its intensity is from ^{205}Bi.

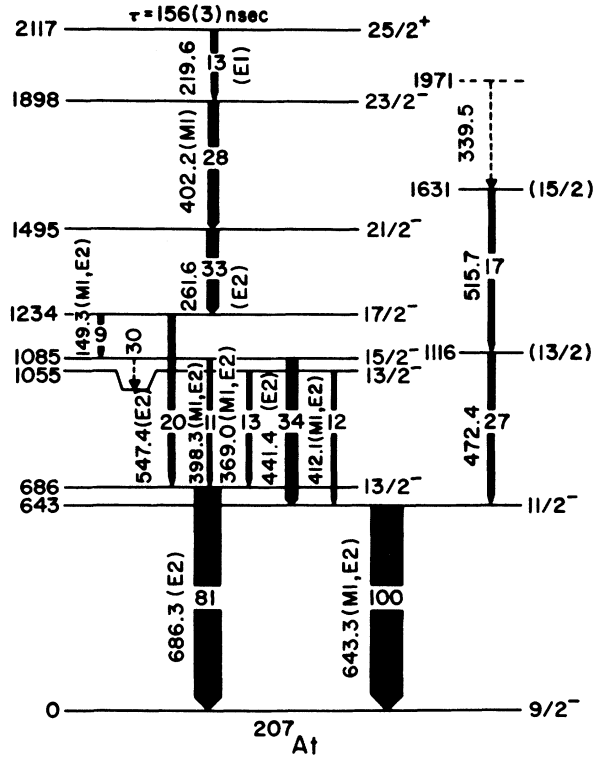

FIG. 3. The level scheme for ^{207}At determined from the present ^{204}Pb(^{6}Li, 3n) γ-ray measurements. The energies of the levels and the γ rays are in units of keV. The γ-ray intensities are normalized to the 643.3 keV yield, which is set equal to 100.

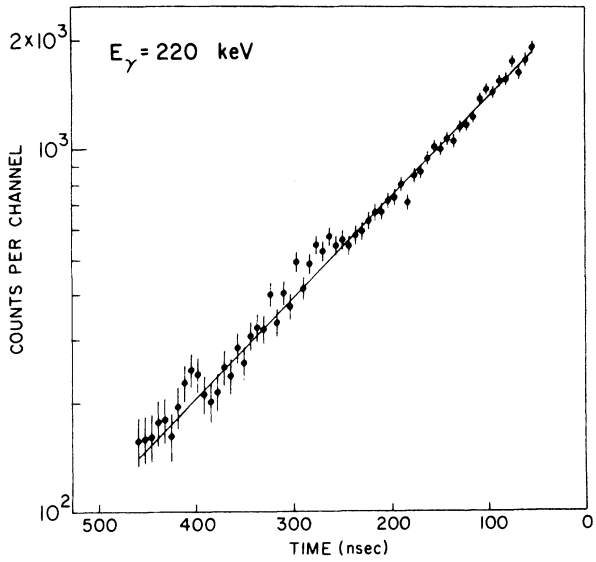

FIG. 4. Results of the time differential lifetime measurement of the 2117-keV $\frac{25^+}{2}$ state obtained from the time spectrum of the 220-keV γ ray. The solid line is a least squares fit to the data, which yielded a mean lifetime of 156(3) ns.

for this isomer was found in the delayed Ge(Li) spectra which showed that all the γ rays involved in the cascade from the 2117-keV level had similar delayed components. From the time differential measurements, it was observed that the 220-keV γ ray had no prompt component. Since the 2117-keV level decays directly via this γ ray, this indicated that the level is isomeric. A least squares fit of a single lifetime to the 220-keV time differential data, shown in Fig. 4, yielded $\tau = 156$ (3) nsec. Time differential measurements for the 261-, 402-, and 441-keV γ rays also yielded lifetimes in excellent agreement with this value. For all other ^{207}At levels, the γ-ray time spectra imply lifetime upper limits of $\tau \leq 8$ nsec.

It was also observed in the time differential measurements, that the 412-keV γ ray was delayed. Since the mean lifetime of the delayed component is consistent with 156 nsec, this suggested a weak branch from the 1085-keV level to the 1055-keV level via an unobserved 30-keV transition. The tentative nature of this assignment is indicated by the dotted γ-ray transition in the level scheme (Fig. 3). The possibility of a weakly populated isomeric state which decays to the 1055-keV level is not ruled out.

The g-factor measurement for the 2117-keV isomer yielded an uncorrected value of $g = 0.295$ (9). The results of the measurements for the 402-keV γ ray are shown in Fig. 5. Corrections for diamagnetism and Knight shift[13] increase this value to 0.30 (1).

The information extracted from the angular distribution measurements is summarized in Table II, where the relative γ-ray intensities and angular distribution A_2 and A_4 coefficients are listed. The deduced γ-ray multipolarities and J^π assignments for ^{207}At are also included in Table II and in the level scheme in Fig. 3. These assingments were obtained from the angular distributions with the assumptions that the states are aligned in low-m substates and that the dominant γ-ray decay proceeds by stretched transitions $J \rightarrow J - L$, where L refers to the γ-ray multipolarity. These features are expected in (HI, xn) fusion evaporation reactions.[14] Lifetime information and conversion coefficients extracted from the delayed γ-ray intensities also aided in these assignments.

The spectroscopic information for the dominant decay cascade shown on the left hand side of Fig. 3 will be discussed first. The intensity of the levels in this cascade decrease in intensity as the energy of the initial state increases. This is characteristic of the population of yrast levels and the subsequent stretched $J \rightarrow J - L$ transitions. The

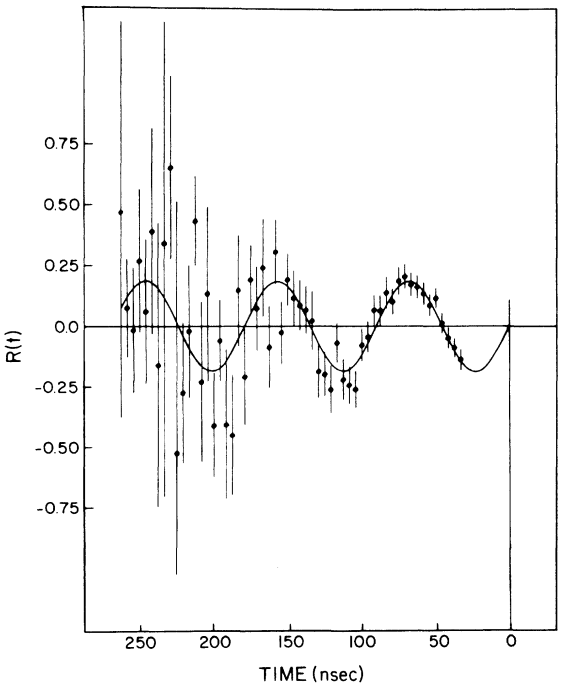

FIG. 5. Results of the perturbed angular distribution g-factor measurement of the 2117-keV $\frac{25}{2}^+$ state in ^{207}At using the 402-keV γ ray. An external magnetic field of 12.6(1) kG was applied. The corrected g factor was found to be 0.30(1).

TABLE II. Results of the angular distribution measurements for ^{207}At.

E_γ (keV)[a]	I_γ[b]	A_2	A_4	$J_i \rightarrow J_f$[c]
149.3	9	−0.33 ± 0.08		$\frac{17}{2}^- \rightarrow \frac{15}{2}^-$
219.6	13	−0.11 ± 0.07	0.1 ± 0.1	$\frac{25}{2}^+ \rightarrow \frac{23}{2}^-$
261.6	33[d]	0.2 ± 0.1	−0.1 ± 0.1	$\frac{21}{2}^- \rightarrow \frac{17}{2}^-$
339.5[e]				
344.3	65	0.00 ± 0.03	−0.09 ± 0.05	
369.0	13	0.1 ± 0.1		$\frac{13}{2}^- \rightarrow \frac{13}{2}^-$
398.3	11	−0.55 ± 0.05		$\frac{15}{2}^- \rightarrow \frac{13}{2}^-$
402.2	28	−0.19 ± 0.03		$\frac{23}{2}^- \rightarrow \frac{21}{2}^-$
412.1	12	−0.68 ± 0.05		$\frac{13}{2}^- \rightarrow \frac{11}{2}^-$
441.4	34	0.21 ± 0.03	−0.09 ± 0.06	$\frac{15}{2}^- \rightarrow \frac{11}{2}^-$
472.4	27	−0.17 ± 0.05		$(\frac{13}{2}) \rightarrow (\frac{11}{2})$
515.7	17	−0.59 ± 0.05	−0.11 ± 0.08	$(\frac{15}{2}) \rightarrow (\frac{13}{2})$
547.4	20	0.27 ± 0.04	−0.06 ± 0.06	$\frac{17}{2}^- \rightarrow \frac{13}{2}^-$
643.3	100	−0.60 ± 0.03	−0.02 ± 0.03	$\frac{11}{2}^- \rightarrow \frac{9}{2}^-$
686.3	81[f]	0.24 ± 0.09	−0.1 ± 0.1	$\frac{13}{2}^- \rightarrow \frac{9}{2}^-$

[a] All γ-ray energies are accurate to ±0.3 keV.

[b] γ-ray intensities are normalized to the 643.3-keV γ-ray yield; unless otherwise noted, intensities are accurate to 10%.

[c] Tentative J^π assignments are denoted by parentheses.

[d] Error in intensity is 20%; this error and the large errors in the A_2 and A_4 coefficients are due to the difficulty in resolving this γ ray from the 260.5 and the 262.8-keV γ rays in ^{205}Pb.

[e] This γ ray is contaminated by a γ ray of the same energy in ^{205}Bi.

[f] The error in the intensity is ±20%; this error and the large errors in A_2 and A_4 coefficients are due to the contamination by the 686.5-keV transition from the radioactive decay of ^{208}At. The angular distribution for the ^{207}At component was extracted by subtracting the radioactive component from the total yield at each angle. The yield of the radioactive component was determined from the yields for the 177.0- and 660.0-keV γ rays and the relative intensities for ^{208}At decay.

least intense cascade, which is indicative of nonyrast levels, is shown on the right side of Fig. 3. The similar large positive A_2 coefficients and small negative A_4 coefficients extracted from the 262, 441, 547, and 686 keV γ-ray angular distributions, identify these γ rays as stretched $J \rightarrow J-2$ $E2$ transitions. The lifetime limits obtained for these γ rays makes $M2$ multipolarities unlikely. For the 149-, 398-, 402-, and 643-keV γ rays, the large negative A_2 coefficients and lifetime limits strongly suggest $J \rightarrow J-1$ transitions of mixed $M1/E2$ multipolarities with negative mixing ratios. Based on a $\frac{9}{2}^-$ ground state for ^{207}At, these multipolarities imply the following J^π assignments: 643-keV $\frac{11}{2}^-$, 686-keV $\frac{13}{2}^-$, 1085-keV $\frac{15}{2}^-$, 1234-keV $\frac{17}{2}^-$, and 1495-keV $\frac{21}{2}^-$. For the 402- and 220-keV γ rays, the deduced multipolarities are $M1/E2$ and $E1$, respectively. The negative A_2 coefficients for both γ rays imply dipole components. In addition, the delayed γ-ray intensities for the 261-, 402-, and 220-keV sequence of γ rays, show that the 220-keV γ ray undergoes very little internal conversion, which can only be explained by an $E1$ multipolarity. The delayed intensities also suggest an $M1/E2$ multipolarity for the 402-keV γ ray. These multipolarities imply that $J^\pi = \frac{23}{2}^-$ and $\frac{25}{2}^+$ for the 1898-keV state and the 2117-keV isomer, respectively. The interpretation of the g-factor results, which will be discussed in the next section, also strongly supports the $\frac{25}{2}^+$ assignment for the 2117-keV isomer.

A definite J^π assignment of $\frac{13}{2}^-$ can also be made for the nonyrast 1055-keV level, which is populated with less intensity than the $\frac{15}{2}^-$ 1085-keV level. The 1055-keV level deexcites via the 412- and 369-keV γ rays to the $\frac{11}{2}^-$ 643-keV and $\frac{13}{2}^-$ 686-keV levels, respectively. The angular distributions and lifetime limits for these γ rays suggest mixed $M1/E2$ multipolarities. Moreover, the

angular distributions of these γ rays and the lifetime limit $\tau \leq 8$ nsec of the unobserved 30-keV transition are consistent with each other only if the 1055-keV level has $J^\pi = \frac{13}{2}^-$.

The γ-ray transitions shown on the right in Fig. 3, which were observed with generally less intensity, appear to involve nonyrast (bandlike) levels. These transitions also decrease in intensity as the energy of the initial state increases, suggesting a stretched γ cascade. The angular distribution coefficients and lifetime limits imply dipole components for both the 472- and 516-keV γ rays, which suggest $J = (\frac{13}{2})$ and $(\frac{15}{2})$ for the 1116- and 1631-keV levels, respectively. The tentative nature of these assignments is denoted by the brackets.

IV. DISCUSSION

The results of the present ^{204}Pb(^{6}Li, $3n$)^{207}At γ-ray measurements are summarized in Tables I and II and in the level scheme of Fig. 3. In the shell-model description with ^{208}Pb as a double closed shell nucleus, the ^{207}At levels involve three-proton-particle and four-neutron-hole configurations of the type $|(\pi)^3 J_p, (\nu)^{-4} J_n; J\rangle$. In Fig. 6, the

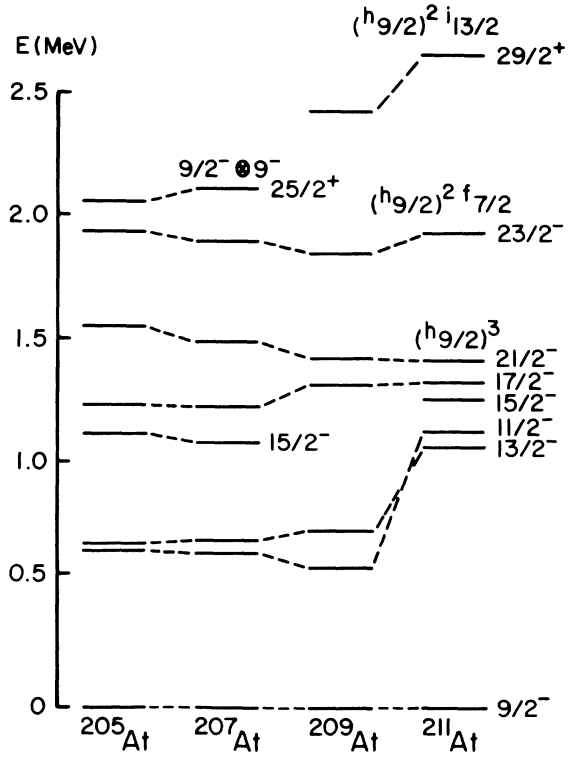

FIG. 6. Yrast levels in ^{205,207,209,211}At. The levels for ^{205,209,211}At were taken from Refs. 7, 4, and 13, respectively.

^{207}At yrast levels are compared with those for ^{209}At and ^{211}At, which have, respectively, $|(\pi)^3 J_p, (\nu)^{-2} J_n; J\rangle$ and $|(\pi^3) J\rangle$ configurations relative to ^{208}Pb. This comparison is used to suggest dominant configurations for the yrast levels in ^{207}At.

The lowest lying excited yrast levels in ^{207}At are the $\frac{11}{2}^-$ and $\frac{13}{2}^-$ levels at 643- and 686-keV, respectively. The large energy reduction of these states relative to yrast $\frac{11}{2}^-$ and $\frac{13}{2}^-$ states in ^{211}At indicates that these levels are predominantly the $(\nu)^{-4}\, 2^+$ excitation of ^{204}Pb at 899 keV coupled to the $(\pi h_{9/2})^3 \frac{9}{2}^-$ ground state configuration of ^{211}At. In ^{209}At,[4,5] the $\frac{11}{2}^-$ and $\frac{13}{2}^-$ yrast levels are reduced in energy also, since the 2^+ state in ^{206}Pb is at 803 keV. Similar energy reductions for the yrast 2^+ states in ^{206,208}Po relative to that for ^{210}Po have been observed.[3,15]

The yrast $\frac{15}{2}^-$ and $\frac{17}{2}^-$ levels in ^{207}At are most likely neutron excitations involving the $(\nu)^{-4}\, 4^+$ state at 1274 keV in ^{204}Pb coupled to the ^{211}At ground state configuration. This is considerably different than that observed in ^{209}At (see Fig. 6). In this nucleus no $\frac{15}{2}^-$ yrast level was observed and the $\frac{17}{2}^-$ yrast level, which is about 100 keV higher than that in ^{207}At, is predominantly a $(\pi h_{9/2})^3 \frac{17}{2}^-$ proton excitation with an inactive $(\nu)^{-2} 0^+$ component. This difference can be understood qualitatively by comparing the ^{204}Pb and ^{206}Pb level schemes. In ^{206}Pb the first excited 4^+ state is 410 keV higher than that in ^{204}Pb. Thus the $(\pi h_{9/2})^3 \frac{17}{2}^-$ proton excitation in ^{207}At should be several hundred keV higher than the yrast $\frac{17}{2}^-$ level.

The systematics of the At yrast levels in Fig. 6 strongly suggest that, similar to ^{209}At, the $\frac{21}{2}^-$ and $\frac{23}{2}^-$ levels in ^{207}At are predominantly $(\pi h_{9/2})^3 \frac{21}{2}^-$ and $(\pi h_{9/2})^2 (\pi f_{7/2}) \frac{23}{2}^-$ proton excitations coupled to the ^{204}Pb ground state $(\nu)^{-4} 0^+$. The yrast systematics in Fig. 6 show that the $\frac{21}{2}^-$ and $\frac{23}{2}^-$ levels are increasing in energy relative to the ground state as the number of neutron holes increases. This feature is also observed in ^{204,206,208}Po for the 8^+ and 6^+ levels, which are known to be predominantly $|(\pi h_{9/2})^2 J, (\nu)^{-n} 0^+; J\rangle$.[15,3]

The $\frac{25}{2}^+$ isomer in ^{207}At has no known comparison level in ^{209}At or ^{211}At. In ^{211}At, the yrast $\frac{25}{2}^+$ state is a $(\pi h_{9/2})^2 (\pi i_{13/2})$ proton excitation at 2617 keV.[16] Based on the ^{209}At level scheme, this state is expected near 2.4 MeV in ^{207}At, which is about 300 keV higher than the observed $\frac{25}{2}^+$ yrast isomer. This suggests that the isomer most likely involves the 9^- neutron excitation in ^{204}Pb near 2.2 MeV. This would be especially interesting because the 9^- states in the even Pb isotopes are known to have very pure $(\nu i_{13/2})^{-1} (\nu f_{5/2})^{-1}$ neutron quasiparticle structures[17] and should provide information

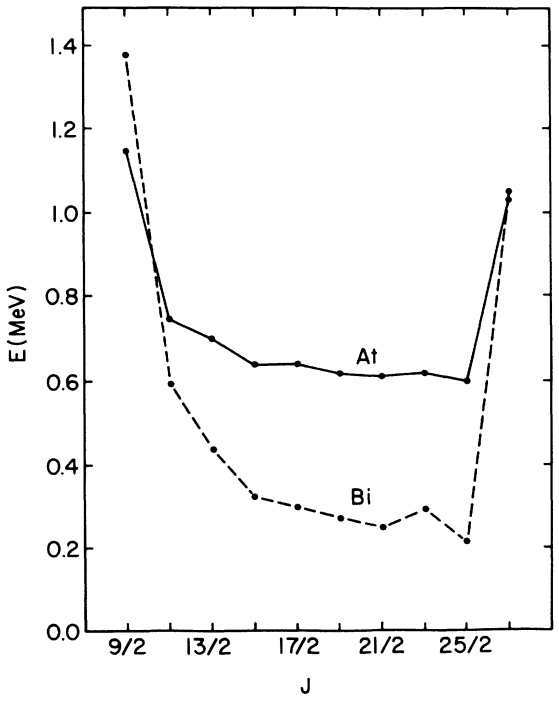

FIG. 7. Calculated relative energies of the $|(\pi h_{9/2})^n \frac{9}{2}^-, (\nu i_{13/2})^{-1}(\nu f_{5/2})^{-1} 9^-; J\rangle$ multiplets for Bi ($n=1$) and At ($n=3$).

on the coupling between the valence $h_{9/2}$ protons and the $i_{13/2}$ and $f_{5/2}$ neutron holes.

The $|(\pi h_{9/2})^3 \frac{9}{2}^-, (\nu i_{13/2})^{-1}(\nu f_{5/2})^{-1} 9^-; \frac{25}{2}^+\rangle$ configuration for the $\frac{25}{2}^+$ isomer in ^{207}At can be checked by a comparison between the observed $g=0.30$ (1) and the value calculated from vector coupling using empirical g factors. This calculation using $g(\nu i_{13/2})^{-1} = -0.155$ (4) extracted from ^{206}Pb,[18] $g(\nu f_{5/2})^{-1} = 0.316$ (12) from ^{207}Pb,[19] and $g(\pi h_{9/2})^3 = 0.917$ (16) from ^{211}At,[13] yields $g=0.264$ (6). This calculated value is in fair agreement with the observed g factor considering that the calculation neglects nonadditive effects and possible admixtures. The nonadditive effects cannot be quantitatively evaluated without detailed knowledge of the structure of the $(\nu)^{-2}0^+$ components; but on the basis of previous g-factor measurements in the Pb region, these effects are expected to be small, on the same order as the experimental error. Contributions to the g factor from possible admixtures should arise primarily from $|(\pi h_{9/2})^2(\pi i_{13/2})\frac{25}{2}^+, (\nu)^{-4}0^+; \frac{25}{2}^+\rangle$ which has a large g factor (~1.1). Nevertheless, the inclusion of this admixture in the wave function for the g-factor calculation still results in an amplitude of 0.98 for the dominant configuration involving the 9^- neutron excitation.

The lifetime result for the $\frac{25}{2}^+ \rightarrow \frac{23}{2}^-$ $E1$ transition in ^{207}At is also consistent with the $|(\pi h_{9/2})^3 \frac{9}{2}^-, (\nu i_{13/2})^{-1}(\nu f_{5/2})^{-1} 9^-; \frac{25}{2}^+\rangle$ interpretation of the $\frac{25}{2}^+$ isomer as well as with the suggested $|(\pi h_{9/2})^2(\pi f_{7/2})\frac{23}{2}^-, (\nu)^{-n}0^+; \frac{23}{2}^-\rangle$ configuration for the $\frac{23}{2}^-$ level. It is expected that a transition between the $\frac{25}{2}^+$ and $\frac{23}{2}^-$ levels would be severely hindered because a single particle transition between the suggested dominant configurations is not possible. Using an internal conversion coefficient of 0.066 for the 220 keV γ ray in ^{207}At,[20] the $B(E1)$ value extracted from the lifetime is $3.57(7)\times10^{-7}$ e^2 fm^2 which is hindered by about a factor of 10^7 relative to Weisskopf estimates. This large hindrance agrees with the above conjecture.

With the above interpretation of the g factor and lifetime measurements the $\frac{25}{2}^+$ state is identified as predominantly $|(\pi h_{9/2})^3 \frac{9}{2}^-, (\nu i_{13/2})^{-1}(\nu f_{5/2})^{-1} 9^-; \frac{25}{2}^+\rangle$. The isomeric nature of the $\frac{25}{2}^+$ yrast state exhibits the interesting feature that it is the lowest member of the $|(\pi h_{9/2})^3 \frac{9}{2}^-, (\nu i_{13/2})^{-1}(\nu f_{5/2})^{-1} 9^-; J\rangle$ multiplet, which has a maximum spin $J_{max} = \frac{27}{2}^+$. This observation agrees with the semiempirical $J_{max}-1$ rule,[21] which predicts that the lowest lying member of a $|(\pi)J_p, (\nu)^{-2}J_n; J\rangle$ three quasiparticle multiplet will have a spin $J = J_{max}-1$. The observation of this feature in the At isotopes suggest that the $J_{max}-1$ rule, which arises from the neutron-hole proton-particle effective interaction, is also valid for $|(\pi)^3 J_p, (\nu)^{-2}J_n; J\rangle$ multiplets involving predominantly seniority-one $(\pi)^3$ configurations. The quantitative aspects of this feature can be understood for the $\frac{25}{2}^+$ isomer, because the simple structure allows the energies of the multiplet to be calculated.

A shell model calculation of the relative energies of the $|(\pi h_{9/2})^3 \frac{9}{2}^-, (\nu i_{13/2})^{-1}(\nu f_{5/2})^{-1} 9^-; J\rangle$ multiplet was made with empirical $\pi h_{9/2}\nu i_{13/2}{}^{-1}$ and $\pi h_{9/2}\nu f_{5/2}{}^{-1}$ particle-hole matrix elements taken from the review article[22] by Schiffer and True. The empirical matrix element $\langle(\pi h_{9/2})^3 \frac{9}{2}^-|V|(\pi h_{9/2})^3 \frac{9}{2}^-\rangle = -0.352$ MeV was extracted from ^{211}At. The results of the calculations (see Fig. 7) show, generally, that the energies of the multiplet decrease slowly with increasing spin J reaching a minimum at $J = J_{max}-1 = \frac{25}{2}^+$. However, for the stretched member $J = J_{max} = \frac{27}{2}^+$, the resulting energy is 435 keV above the $\frac{25}{2}^+$ state. Thus the calculation is able to reproduce the feature that the $\frac{25}{2}^+$ state is the lowest member of this multiplet.

This result can be understood by examing the particle-hole matrix elements $\langle \pi h_{9/2}\nu i_{13/2}{}^{-1} j|V|\pi h_{9/2}\nu i_{13/2}{}^{-1} j\rangle$ and $\langle \pi h_{9/2}\nu f_{5/2}{}^{-1} j|V|\pi h_{9/2}\nu f_{5/2}{}^{-1} j\rangle$ as a function of the spin j. Both sets of these matrix elements[22] are repulsive showing a weak j dependence except for the maximum and the minimum spin j. For these extremum spins the matrix elements are enhanced considerably, becoming more repulsive by about

a factor of 2 because the overlap of the wave functions is maximized. (This is just the analog of the neutron-proton two-body matrix elements where maximum overlap produces the strongest attractive force.) Furthermore, the matrix elements indicate that the enhancement is greater for particle-hole orbitals with large orbital angular momentum such as $\pi h_{9/2}\nu i_{13/2}^{-1}$. Thus for the $\frac{27}{2}^+$ state the strongly repulsive $\langle \pi h_{9/2}\nu i_{13/2}^{-1} j_{\max} = 11^- | V | \pi h_{9/2}\nu i_{13/2}^{-1} 11^- \rangle$ matrix element dominates the particle hole interactions, pushing this state 435 keV above the $\frac{25}{2}^+$ member.

It is interesting to compare the splitting of the $|(\pi h_{9/2})\frac{9}{2}^-, (\nu i_{13/2})^{-1}(\nu f_{5/2})^{-1} 9^-; \frac{25}{2}^+\rangle$ multiplet in the odd-mass Bi isotopes with that discussed for At. As expected, the calculation for Bi gives a similar J dependence (see Fig. 7), although the average interaction energy is lower because there is only one proton. The calculated $\frac{25}{2}^+$ state is the lowest member of the multiplet with the $\frac{27}{2}^+$ state pushed 840 keV higher than the $\frac{25}{2}^+$ state, which makes the Bi splitting about twice the value in At. The splitting in At is modified by the two additional protons, which increase the number of neutron-proton interactions. This tends to smooth the multiplet J dependence and thus reduces the splitting. Although the experimental information on the Bi multiplet is not well defined, recent ^{203}Bi (Ref. 1) and ^{205}Bi (Ref. 2) studies suggest yrast $\frac{25}{2}^+$ and $\frac{27}{2}^+$ states, which are split by 689 and 640 keV, respectively. These results are not inconsistent with the calculated value of 840 keV, since the calculation has neglected the $(\nu)^{-4}0^+$ components in ^{203}Bi and the $(\nu)^{-2}0^+$ components in ^{205}Bi.

The $J_{\max} - 1$ rule also appears to be valid for those yrast states in ^{207,209}At which are identified as $J = 2^+, 4^+$ Pb core excitations coupled to the ^{211}At ground state. This is also true in ^{207}Bi (Ref. 23) for states that are $(\nu)^{-2} J = 2^+, 3^+, 4^+$, and 7^- excitations of ^{206}Pb coupled to an $h_{9/2}$ proton. Similarly in ^{203}Bi (Ref. 1) and ^{205}Bi,[2] the $\frac{11}{2}^-$ member of the $|(\pi h_{9/2})\frac{9}{2}^-, (\nu)^{-n} 2^+; J\rangle$ multiplet is lowest. For ^{207}Bi, a shell model calculation[23] using a weak coupling basis of $\pi h_{9/2} \otimes (^{206}\text{Pb})$ and empirical two body matrix elements predicts the $J_{\max} - 1$ feature for all of the multiplets.

In Fig. 6 the ^{205}At yrast level scheme[7] is also compared with those for ^{207,209,211}At. The most striking feature is that the yrast level schemes for ^{207}At and ^{205}At are nearly identical. In fact, the $\frac{25}{2}^+$ state in ^{205}At is also isomeric with a mean lifetime[7] of $\tau = 92$ nsec and it decays, as in ^{207}At, via a highly hindered $E1$ transition. This similarity can be understood qualitatively, since both the ^{202}Pb and ^{204}Pb level schemes are also nearly identical. The systematics for these At isotopes involving neutron-hole cores can be compared to recent results[24] on the ^{213}At nucleus, which involves a ^{210}Pb neutron-particle $(\nu)^2$ core. As can be seen by the At level schemes shown in Fig. 6, no significant collectivity in terms of yrast band structure has developed at these excitation energies in the At isotopes down to $N = 120$.

This study was supported in part by the National Science Foundation.

---

*Present address: Indiana University Cyclotron Facility, Bloomington, Indiana 47405.

†Present address: Cyclotron Institute, Texas A&M University, College Station, Texas 77843.

[1] H. Hübel, A. Kleinrahm, C. Günther, D. Mertin, and R. Tischler, Nucl. Phys. A294, 177 (1978).

[2] R. Brock, C. Günther, H. Hübel, A. Kleinrahm, D. Mertin, P. Meyer, and R. Tischler, Nucl. Phys. A278, 45 (1977).

[3] H. Beuscher, D. R. Zolnowski, D. R. Haenni, and T. T. Sugihara, Phys. Rev. Lett. 36, 1128 (1976).

[4] T. P. Sjoreen, G. Schatz, S. K. Bhattacherjee, B. A. Brown, D. B. Fossan, and P. M. S. Lesser, Phys. Rev. C 14, 1023 (1976).

[5] I. Bergström, C. J. Herrlander, Th. Lindblad, V. Rahkonen, K.-G. Rensfelt, and K. Westerberg, Z. Phys. A 273, 291 (1975).

[6] T. P. Sjoreen, U. Garg, and D. B. Fossan, Phys. Lett. 76B, 397 (1978).

[7] T. P. Sjoreen, D. B. Fossan, U. Garg, A. Neskakis, A. R. Poletti, and E. K. Warburton, Proceedings of the International Symposium on High-Spin Phenomena in Nuclei, Argonne, Illinois, 1979 (ANL Report No. ANL/PHY-79-4), p. 469.

[8] A. R. Poletti, T. P. Sjoreen, D. B. Fossan, U. Garg, A. Neskakis, and E. K. Warburton, Phys. Rev. C 20, 1768 (1979).

[9] J. Blomqvist, I. Bergström, C. J. Herrlander, C. G. Lindén, and K. Wikström, Phys. Rev. Lett. 38, 534 (1977).

[10] M. R. Schmorak, Nucl. Data Sheets 22, 487 (1977).

[11] T. P. Sjoreen, U. Garg, and D. B. Fossan, Bull. Am. Phys. Soc. 21, 986 (1976); 22, 996 (1977).

[12] O. Häusser, T. K. Alexander, J. R. Beene, E. D. Earle, A. B. McDonald, F. C. Khanna, and I. S. Towner, Nucl. Phys. A273, 253 (1976).

[13] H. Ingwersen, W. Klinger, G. Schatz, and K. Witthuhn, Phys. Rev. C 11, 243 (1975).

[14] J. O. Newton, in *Nuclear Spectroscopy and Reactions*, Part C, edited by J. Cerny (Academic, New York, 1974), p. 185.

[15] K. Wikström, I. Bergström, J. Blomqvist, and C. J. Herrlander, Phys. Scr. 10, 292 (1974).

[16] I. Bergström, B. Fant, C. J. Herrlander, K. Wikström, and J. Blomqvist, Phys. Scr. 1, 243 (1970).

[17] M. Pautrat, G. Albouy, J. C. David, J. M. Lagrange,

N. Poffé, C. Roulet, H. Sergolle, J. Vanhorenbeeck, and H. Abou-Leila, Nucl. Phys. A201, 449 (1973); A201, 469 (1973).
[18]K. Nakai, B. Herskind, J. Blomqvist, A. Filevich, K.-G. Rensfelt, J. Sztarkier, I. Bergström, and S. Nagamiya, Nucl. Phys. A189, 526 (1972).
[19]F. J. Schroeder and T. Toschinski, J. Phys. Soc. Jpn. Suppl. 34, 271 (1973).
[20]R. S. Hager and C. E. Seltzer, Nucl. Data A4, 1 (1968); O. Dragoun, Z. Plajner, and F. Schmutzler, *ibid.* A9, 119 (1971).
[21]L. K. Peker, Yad. Fiz. 4, 27 (1966) [Sov. J. Nucl. Phys. 4, 20 (1967)].
[22]J. P. Schiffer and W. W. True, Rev. Mod. Phys. 48, 191 (1976).
[23]I. Bergström, C. J. Herrlander, P. Thieberger, and J. Blomqvist, Phys. Rev. 181, 1642 (1969).
[24]T. P. Sjoreen, U. Garg, and D. B. Fossan, Phys. Rev. C 21, 1838 (1980).